Preprints.org

Article

Advances in Room Temperature of Indium Aluminum Nitride InAlN Deposition via Co-Sputtering DC for Solar Energy Applications

Juan David Cañón Bermudez and Luis Fernando Mulcué-Nieto [*]

Article

Advances in Room Temperature of Indium Aluminum Nitride InAlN Deposition via Co-Sputtering DC for Solar Energy Applications

Juan David Cañón Bermudez [1,2] and Luis Fernando Mulcué-Nieto [1,3,*]

[1]　Universidad Nacional de Colombia Sede Manizales, Carrera 27 # 64-60, Manizales, Caldas, Colombia.; lfmulcuen@unal.edu.co

[2]　Escuela de Ciencias Básicas, Tecnologías e Ingenierías, Universidad Nacional Abierta y a Distancia UNAD, Diagonal 25 F Carrera 23, Dosquebradas Colombia, 691001; jdcanonb@unal.edu.co

[3]　Departamento de Física y Matemática, Universidad Autónoma de Manizales, Manizales, Caldas, Antigua Estación del Ferrocarril, Colombia

*　Correspondence: lfmulcuen@unal.edu.co

Abstract: The study addresses the fabrication of indium aluminum nitride (InAlN) layers by DC co-sputtering at room temperature, highlighting their potential in optoelectronic and solar cell applications. Experiments were carried out with different powers for the aluminum target, observing changes in the stoichiometry and material properties. XPS and AES analysis confirmed the variation in indium and aluminum concentration, directly affecting bandgap and electrical properties such as mobility and free carrier concentration. The layers showed smooth surfaces with low roughness, suitable for high efficiency interfaces. This method promises to reduce costs and improve the accessibility of efficient solar technologies based on InAlN semiconductor alloy.

Keywords: InAlN solar cells; co-sputtering DC; room temperature; optical properties; morphological properties; low-cost synthesis; Indium Aluminum Nitride

1. Introduction

Indium aluminum nitride (InAlN) emerges as a promising semiconductor material, standing out for its tunable direct bandgap between 0.64eV and 6.2eV depending on its stoichiometric composition [1], [2], [3]. This feature, together with its remarkable radiation resistance [4] and exceptional chemical stability, positions InAlN as an ideal candidate for the fabrication of high-efficiency solar cells [5]. However, the synthesis of high quality InAlN layers represents a significant challenge, especially when seeking to reduce costs through room temperature fabrication processes [6].

Traditionally, the synthesis of InAlN by sputtering requires temperatures above 200°C to facilitate the reaction between nitrogen, indium and aluminum atoms, thus promoting the formation of the compound [7], [8]. These thermal conditions not only favor atomic mobility on the substrate, improving nucleation and thus the crystalline structure of the resulting layer, but are also crucial to avoid the formation of polycrystalline or amorphous structures [3]. In addition, these low structural quality layers usually exhibit a higher amount of electron-hole pair recombination centers, which is adverse to the efficiency of a solar cell.

To date, the scientific literature has not reported obtaining InAlN films with wurzite-type crystal structure and preferential c-plane orientation fabricated at room temperature. Therefore, the development of a method that allows the synthesis of InAlN layers at room temperature, maintaining optimal properties for applications in optoelectronic devices, may represent a significant advance towards the reduction of production costs.

Additionally, the choice of sputtering type, either RF (Radio Frequency) or DC (Direct Current), plays a crucial role in the quality of the synthesized InAlN. Traditionally, RF sputtering has been preferred for the fabrication of InAlN [6], [9], [10] due to its ability to prevent charge accumulation

on the indium target, thus facilitating the deposition of layers with high indium concentration. In contrast, DC sputtering, despite being more economical, faces significant challenges, such as the difficulty in maintaining a high indium concentration in the layers due to arcing, process disruption, and non-uniform target wear.

In this context, our research focuses on overcoming these challenges by developing a method using a DC co-sputtering system for the fabrication of InAlN layers at room temperature. This approach represents a step forward in reducing the costs associated with their production, thus opening new possibilities for the implementation of more affordable and efficient solar technologies.

2. Materials and Methods

The InAlN films were deposited by a DC magnetron sputtering process. For this purpose, indium (99.99% purity) and aluminum (99.999% purity) targets, both 2 inches in diameter, were used. Argon and nitrogen gases were used as inert and reagent gases, respectively. The separation between the target and the substrate was 8 cm. The gas ratio was Ar:N2 = 2:8 sccm, with a base pressure of 1E-7 Torr and an operating pressure of 10 mTorr. The substrate temperature was maintained at room temperature, with a total deposition time of 10 min. Different powers were experimented with for the aluminum target, specifically 60W, 100W, 140W and 180W, while the power for the indium target was kept constant at 20W. Glass was used as substrate after cleaning with isopropyl alcohol.

The chemical compositions and atomic concentrations of In, Al and N in the layers were analyzed by X-ray photoelectron spectroscopy (XPS) and Auger spectroscopy (AES) using an AES-XPS PHI 548 system with Al Ka radiation source (1486.6 eV). Figure 1 illustrates the schematic of the growth system and the setup for XPS characterization. XPS measurements were performed in situ, eliminating the need for carbon calibration. To determine the electrical properties of the layers, Hall effect measurements were performed using an ECOPIA HMS-5000 system in Van der Pauw configuration. Additionally, UV-Vis spectroscopy was used to determine the absorption coefficient of the layers and compare it with other semiconducting materials. The morphological properties of the layers were investigated by atomic force microscopy AFM.
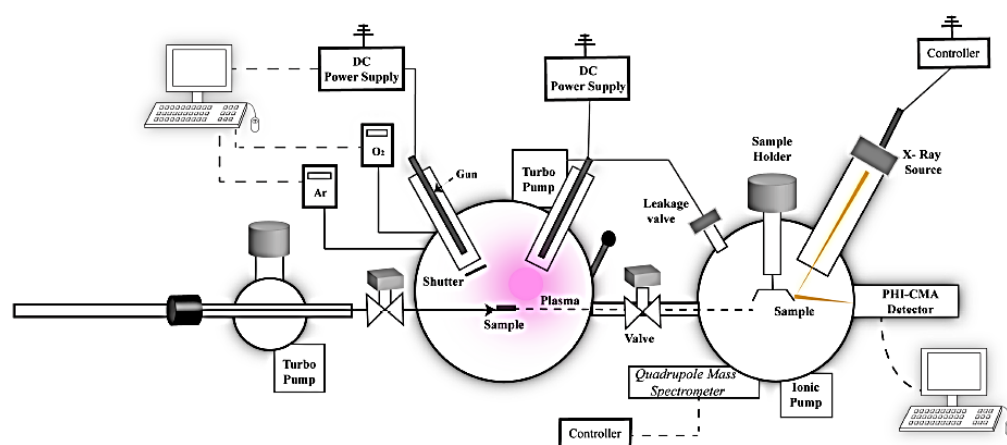

Figure 1. Schematic of the synthesis equipment and characterization stage [11].

3. Results and Discussion

3.1. Chemical Properties

3.1.1. AES Auger Electron Spectroscopy (AES)

The analysis of the AES spectrum in Figure 2 confirmed that all samples show characteristic peaks of indium (In), nitrogen (N), oxygen (O) and carbon (C) atoms. Specifically, the indium peak was recorded at 408eV, corresponding to the MNN transition. The nitrogen peak appeared at 386eV, associated with the KLL transition [12]. Although a peak for aluminum was anticipated at 1390eV, corresponding to the LMM transition, this was not detectable in the measurement range employed.

In addition, small peaks for oxygen and carbon were observed, indicative of slight contamination in the deposition chamber. A peak at 366eV was also observed suggesting the presence of chemical effects related to the covalent bond between indium and nitrogen, confirming the formation of InN. Binary InN is estimated to be stoichiometric from the height ratios of the In/N peaks in the spectrum.
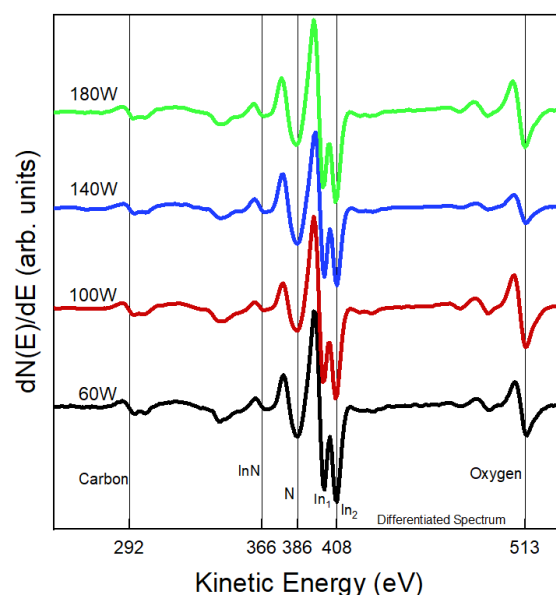

Figure 2. AES Spectrum of InAlN Films: Identification of Elements and Evidence of InN Formation.

3.1.2. X-Ray Photoelectron Spectroscopy (XPS)

To complement the chemical analysis, the survey spectrum in Figure 3 obtained by XPS reveals the presence of five chemical elements: oxygen (O), indium (In), nitrogen (N), and aluminum (Al). The peaks identified in the survey spectrum correspond to the binding energies O1s at 531.4 eV, In3d5/2 at 444.5 eV, N1s at 396.6 eV and Al2p at 73.7 eV [13], [14]. It is important to highlight that, through this XPS analysis, it was possible to identify aluminum atoms in the samples, a result that had not been possible by means of (AES) previously used.
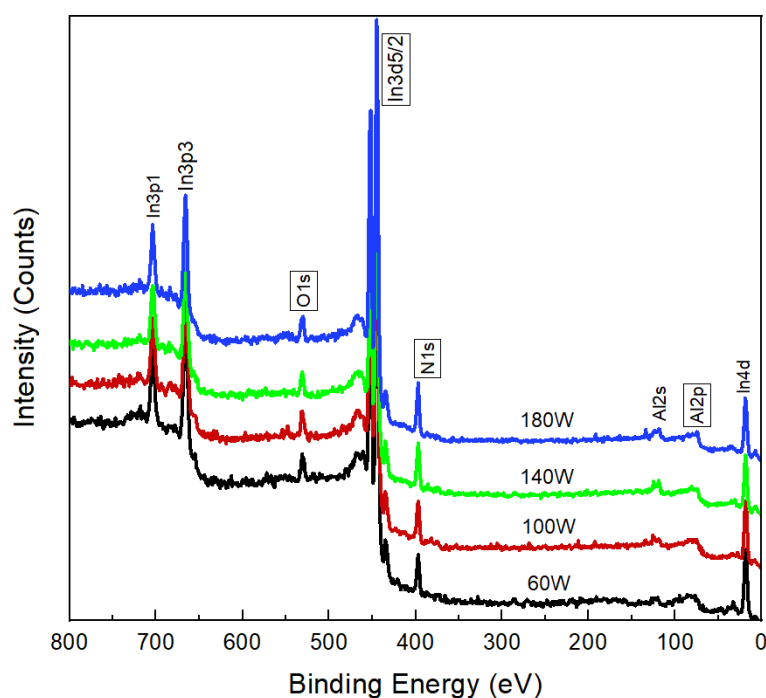

Figure 3. XPS spectra of InAlN layers. Identification of Oxygen, Indium, Nitrogen and Aluminum.

Figure 4 illustrates the high-resolution spectra corresponding to the Al2p, In3d5/2 and N1s peaks of the samples fabricated under various deposition powers. From the spectral data, an increase in the intensity of the Al2p and N1s peaks is observed with increasing power applied to the target. This phenomenon suggests an increased incorporation of aluminum and nitrogen into the film, which is consistent with the formation of aluminum nitride (AlN), evidenced by the increase of the N1s peak. On the other hand, the intensity of the In3d5/2 peak decreases, indicating a reduction in indium concentration in the films as the power is increased. These results point to a modification in the chemical composition of the films, favoring the formation of AlN to the detriment of indium incorporation.
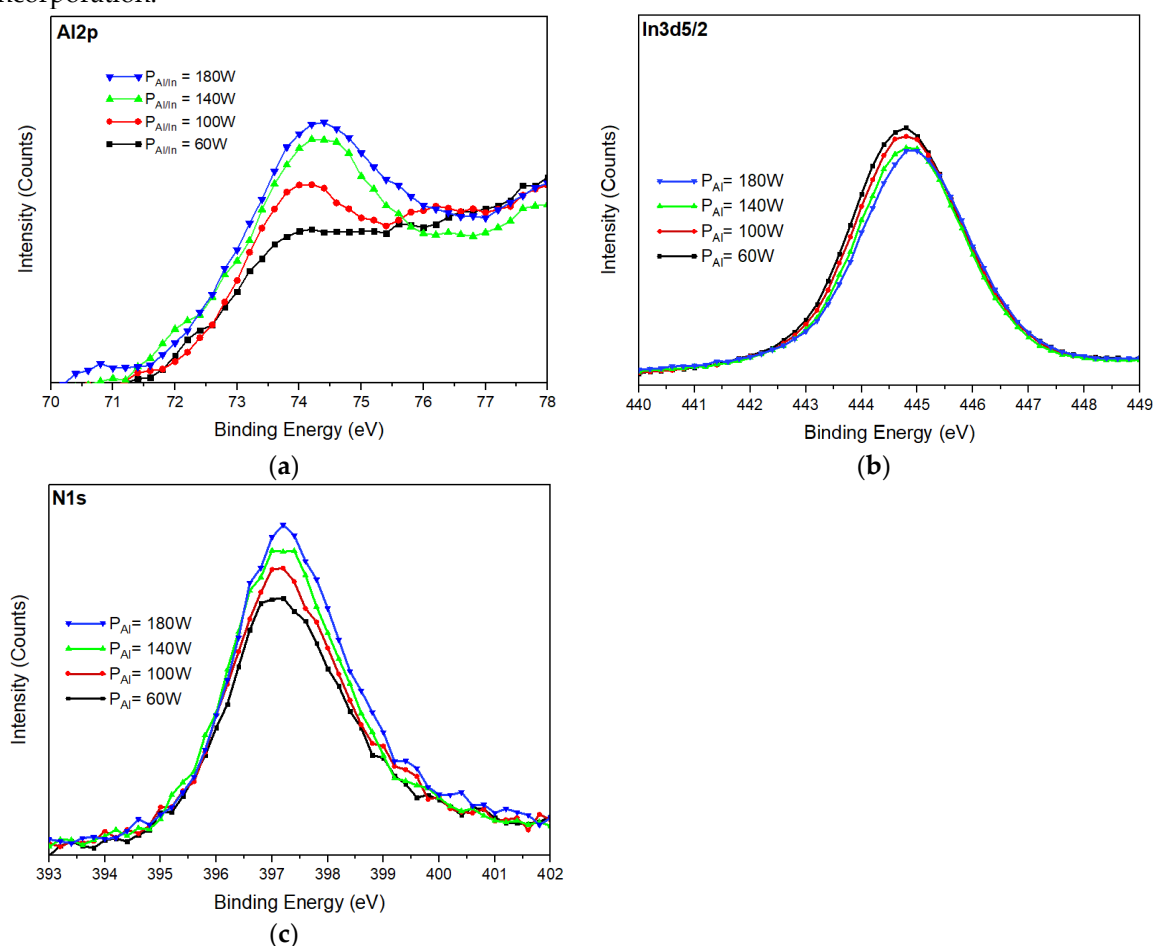

Figure 4. Variation of high-resolution spectra of (a) Al2p; (b) In3d5/2; and (c) N1s peaks as a function of target power.

To determine the chemical nature of the nitrogen bonds in the samples, a mathematical deconvolution of the high-resolution XPS spectra corresponding to the N1s peak was carried out. This deconvolution was performed using Gaussian functions and Shirley-type baseline fits. The results obtained are presented in Figure 4, which shows the deconvolution of the N1s peak for samples prepared under different deposition powers.

In the spectra of the N1s peak, two subpeaks are clearly identified, corresponding to the N-In and N-Al bonds, with binding energies of 396.4 and 399.2 eV, respectively [15], [16], [17]. Detailed deconvolution analysis indicates that, with increasing target power, the subpeak corresponding to N-Al increases in intensity, while the N-In subpeak decreases. This behavior suggests an increased formation of AlN and a reduction in the presence of InN within the semiconducting material.
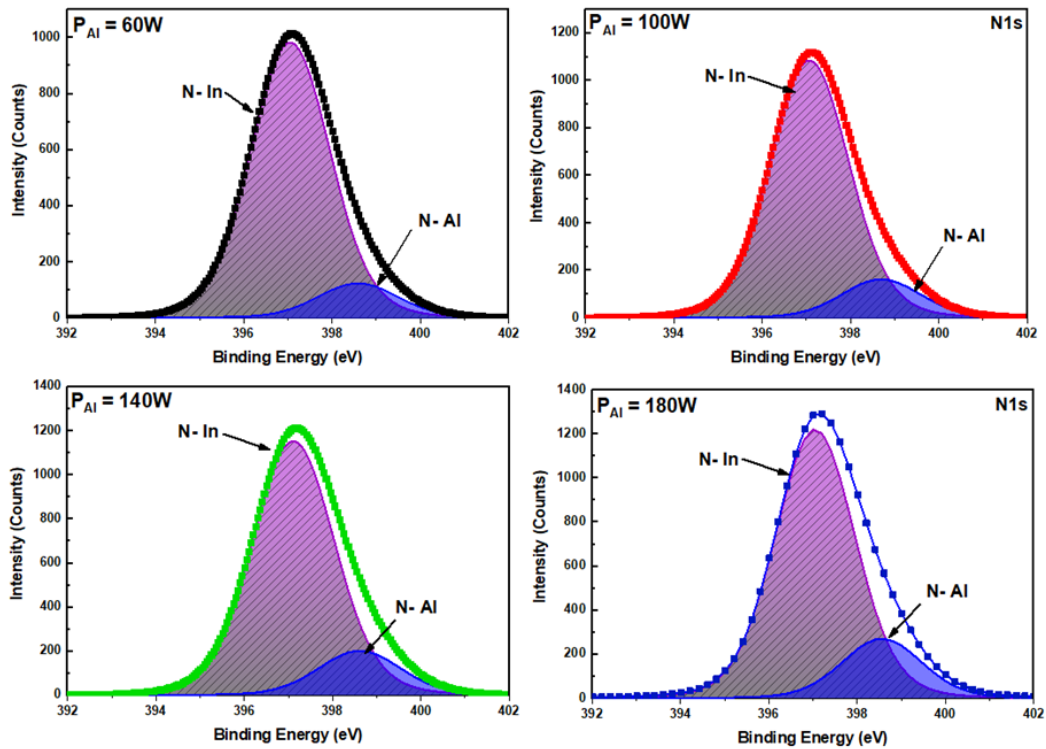
Figure 5. Characterization of N-In and N-Al bonds by deconvolution of XPS spectra of the N1s peak.

Quantification of the ratio of N-In and N-Al bonds was performed by deconvolution of the N1s peak in the XPS spectra of each sample. This analysis allowed us to determine the stoichiometry of the samples and to examine how this varies as a function of the power applied to the aluminum target. The results of this study are summarized in Table 1, which shows the evolution of the chemical formula of InAlN with power variation. A 6% variation in stoichiometry is observed, which is a good result considering that it is a DC co-sputtering process at room temperature.

Table 1. Changes in the chemical composition of InAlN in relation to the applied power.

Power applied to the aluminum target (W)	Formula
60	$In_{0.88}Al_{0.12}N$
100	$In_{0.87}Al_{0.13}N$
140	$In_{0.85}Al_{0.15}N$
180	$In_{0.82}Al_{0.18}N$

Figure 6 shows a comparative analysis of how the power applied to the aluminum target affects the InAlN stoichiometry using DC co-sputtering at room temperature and holding the indium target power constant. This study is contrasted with previous research using RF co-sputtering at temperatures above 300°C, where the indium target power was also held fixed. The results indicate that the use of a room temperature DC system is feasible and allows the stoichiometry of InAlN to be effectively modified. This method significantly reduces fabrication costs, which is crucial for the mass production of optoelectronic devices.
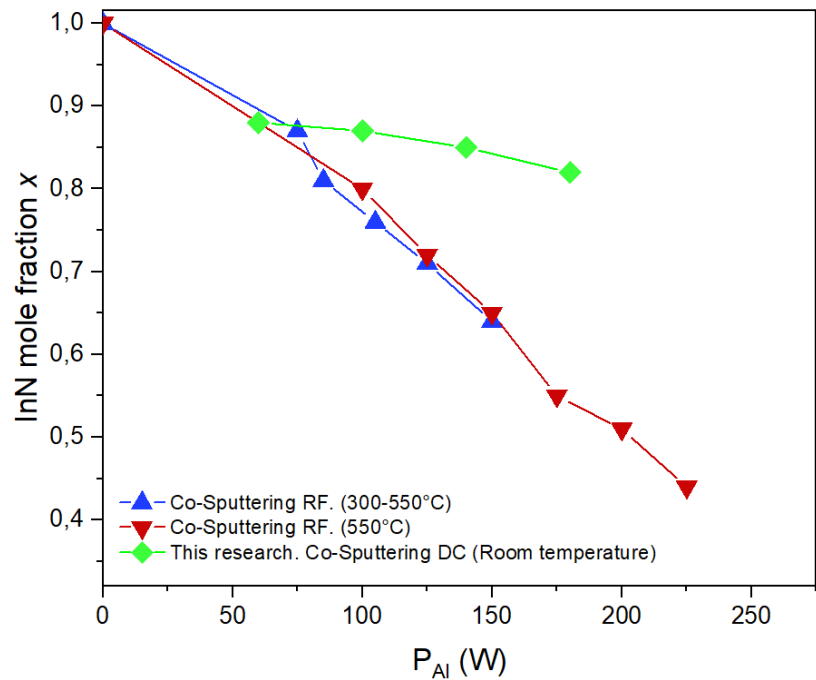
Figure 6. Variation of InN and AlN mole fractions with target power [6], [18].

3.2. Morphological Properties

3.2.1. Atomic Force Microscopy (AFM).

Morphological properties were analyzed by atomic force microscopy (AFM). This morphological analysis provided quantitative data as shown in Table 2. In this table it is observed that as the aluminum target power increases, the thickness of the layer increases and thus its deposition rate.

Table 1. Variation of InAlN Thickness and Deposition Rate as a Function of Aluminum Blank Power.

Power applied to aluminum target (W)	Thickness (nm)	Deposition rate (nm/min)
60	63.523 ± 24	3.59
100	72.093 ± 19	3.70
140	78.938 ± 33	4.09
180	85.092 ± 16	4.11

A surface area of $4 \mu m^2$ was analyzed on each sample to obtain a detailed representation of the morphology. In Figure 7, 3D images obtained by AFM are presented. These images reveal very smooth surface textures, which is characteristic of the sputtering technique.
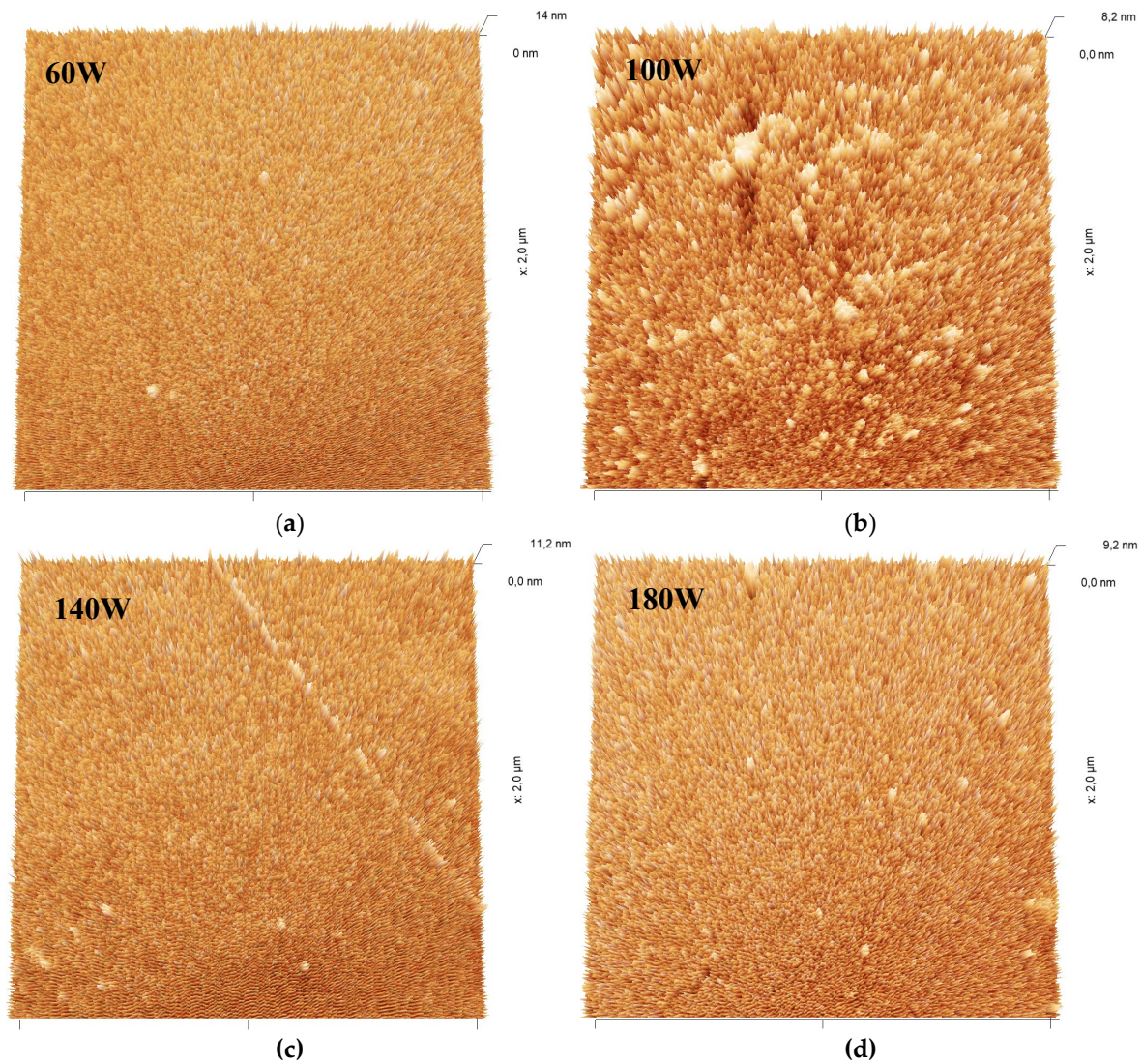
Figure 7. 3D AFM Images of InAlN Layers Fabricated at Different Sputtering Powers. (a) 60W; (b) 100W; (c) 140W; (d) 180W;.

From the statistical analysis of the previous images, Figure 8a was produced, which illustrates the root mean square (RMS) roughness of the samples as a function of the power applied to the aluminum target. This RMS measure reflects the standard deviation of the height distribution of the analyzed surfaces. In general terms, the samples exhibit exceptionally smooth surfaces, with roughness values below 3nm. There is some tendency that as the aluminum target power increases the RMS roughness tends to decrease. Something interesting in this research is that very low roughness values were obtained compared to other samples as observed in Figure 8b [1], [3], [9], [13], [13], [16], [19] a low roughness is desirable for the fabrication of interfaces with low defect density [20] which is useful for the improvement of high efficiency solar cells.
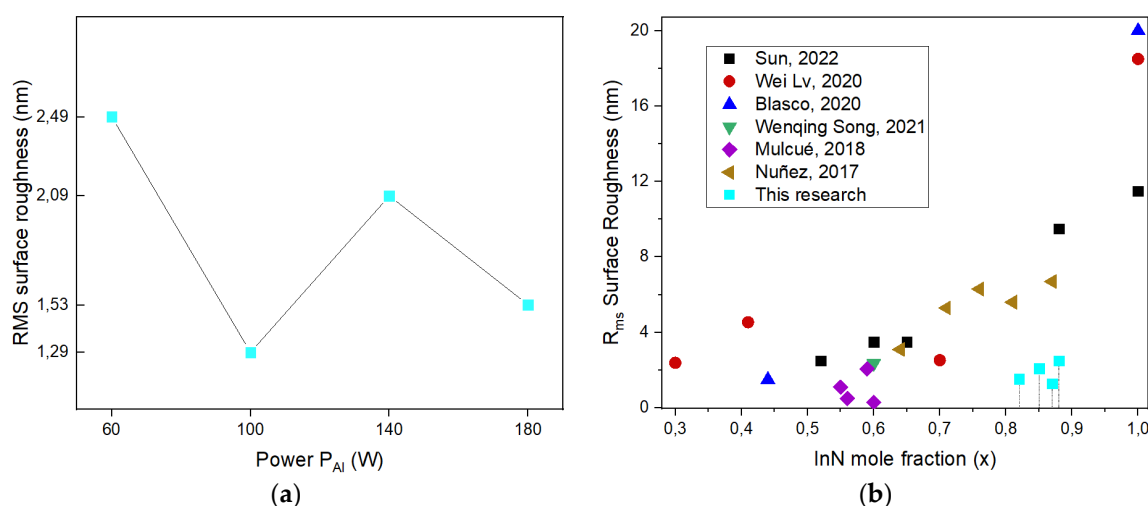
Figure 8. (a) Roughness of InAlN surfaces obtained at different Sputtering Powers; (b) Roughness obtained for different InAlN stoichiometries obtained in different investigations.

To analyze the peak height distribution of the samples, a threshold was used to differentiate the grains from the background by classifying points above the threshold as grains and the rest as background. Figure 9 shows the peak height distribution plot on the surfaces of the samples obtained at different sputtering powers.
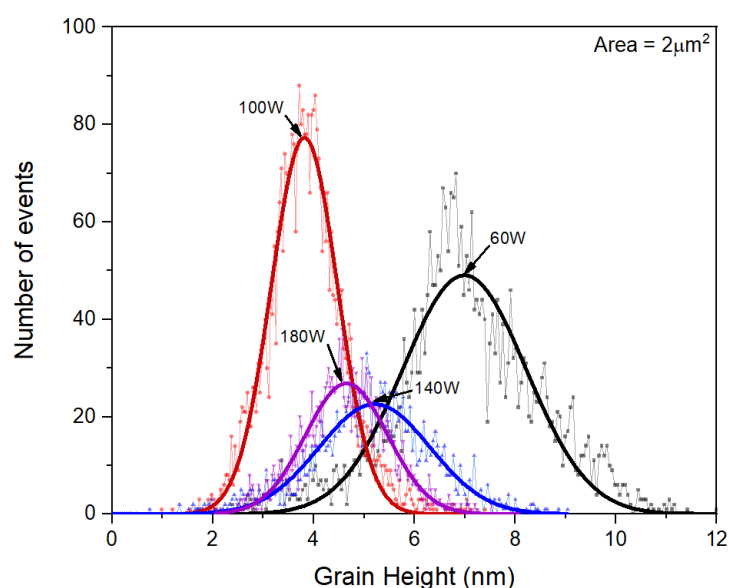

Figure 9. Influence of Sputtering Power on the Morphology of InAlN Surfaces.

In the analysis of the height distribution, notable variations were detected in the predominant grain height for each sample. The sample at 60W reached a predominant height of 7.02nm, in contrast to that at 100W, which recorded a considerably lower height of 3.80nm. When the power was raised to 140W and 180W, the most frequent heights were at 5.25nm and 4.70nm, respectively. However, no direct relationship was established between the predominant height and the power applied to the aluminum target.

The sample at 100W showed the lowest dispersion in peak heights, with values close to an average, which could explain its reduced roughness; however, the existence of numerous peaks, 3725 in the analyzed area, suggests a lower homogeneity in the sample. In contrast, the sample at 60W revealed the greatest dispersion in grain heights, which justifies its high root mean square roughness compared to the other samples.

The samples at 140W and 180W, with 1425 and 1848 peaks respectively, exhibit high dispersion in heights, increasing the roughness. Despite this, the lower number of peaks, compared to other samples, suggests a higher homogeneity, crucial for the efficiency of devices such as solar cells. This uniformity obtained at room temperature could improve the electrical performance for electrical contacts in photovoltaic devices.

3.3. Optical Properties

3.3.1. UV-Vis Spectroscopy

The optical properties of semiconductor layers with various stoichiometries were analyzed using UV-Vis spectroscopy. In this study, the optical transmittance of the samples was evaluated over a range of energies from 1.5 to 4.0eV, spanning both the visible and ultraviolet spectra. The results of these measurements are presented in Figure 10. The figure shows that the samples exhibit a high transmittance in the near infrared. However, this transmittance decreases progressively in the visible spectrum, from the red to the violet. Furthermore, it is highlighted that an increase in target power, leading to a higher proportion of AlN in the sample, results in an increase in transmittance.
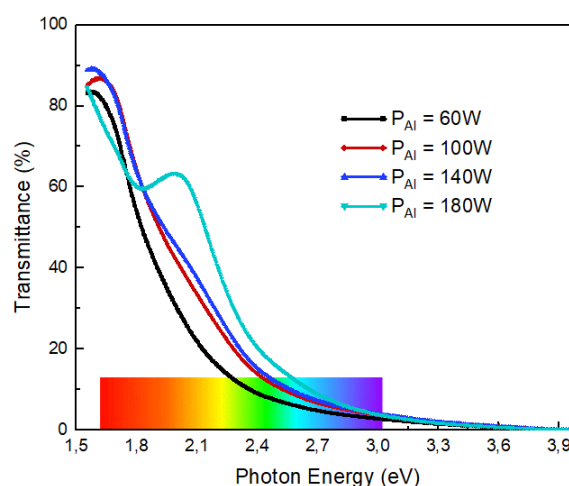

Figure 10. Optical Transmittance of InAlN Layers as a Function of Target Power.

Figure 11 illustrates the absorption coefficient of the samples as a function of photon energy. It is observed that the absorption coefficient is highest in the sample fabricated at the lowest target power and decreases as the power increases. This behavior suggests that the absorption of light by the semiconductor material decreases with increasing AlN content.
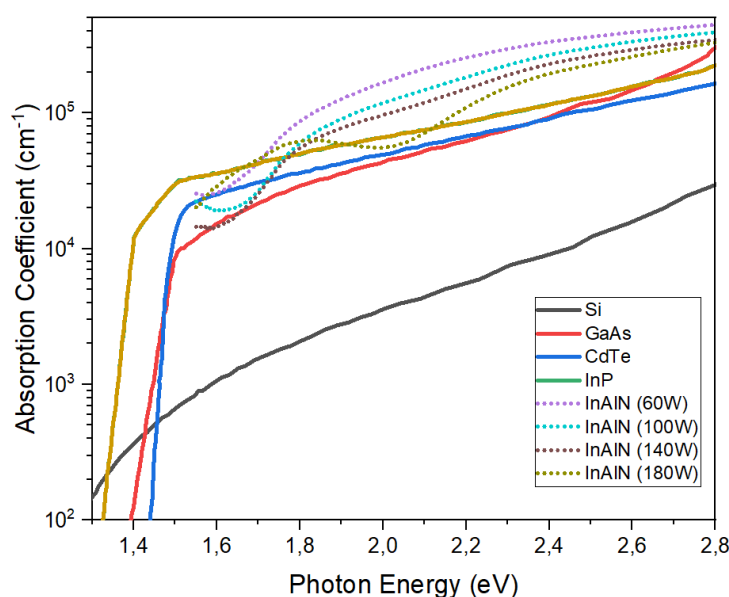
Figure 11. Variation of Absorption Coefficient with Photon Energy as a Function of Target Power in InAlN Layers [21].

To determine the bandgap of the samples, the Tauc method was used, which involves plotting $(\alpha h v)^2$ as a function of photon energy, where α represents the absorption coefficient and $h v$ the photon energy [22], [23]. Figure 12 exhibits the results obtained, showing that the bandgap ranges between 1.8 and 2.0eV as the power of the aluminum target is varied. These values lie within the visible spectrum, specifically in the red-orange range. Furthermore, it is observed that the bandgap increases with increasing target power, which is consistent with theory [3].

The bandgap values obtained are comparable with those of materials such as CdTe (1.48eV) and CdS (2.4eV) [24], [25], commonly used as absorber layer and window layer in solar cells, respectively. This suggests that InAlN alloy fabricated at room temperature by DC sputtering could be useful in such devices.

The explanation for these bandgap values is found in the high working pressure of 10mTorr used during the deposition process, which reduces the kinetic energy of the incident atoms on the substrate and complicates the formation of a more ordered crystalline structure, thus increasing the optical bandgap of the material. Figure 12 also highlights the presence of the Urbach tail in all samples attributable to disordered potentials [2]. However, the sample fabricated at 180W shows a particular shape of this tail, attributable to the distribution of available states within the bandgap, originated by structural defects.
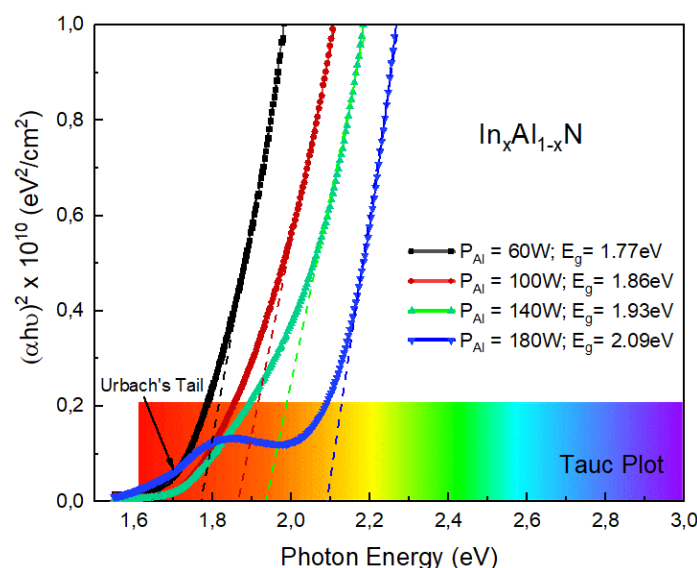
Figure 12. Determination of the Bandgap of InAlN Layers by the Tauc Method and its Variation with Target Power.

3.4. Electrical Properties

3.4.1. Hall Effect

The concentration of free carriers (n) in the InAlN layers was determined using the Hall Effect method. Figure 13 illustrates how n varies as a function of the power applied to the aluminum target. It is observed that n decreases as the power increases, reflecting a reduction in the amount of carriers in the conduction band. This trend is explained by the fact that increasing the power decreases the indium (In) content in the InAlN layers. This decrease in the carrier concentration is attributed to the decrease in Fermi energy with respect to the conduction band edge [26].

The obtained values of n range from 3.1E20 to 1.5E20, figures that, although high, are within the range reported in the literature for this type of semiconductors fabricated by sputtering [1], [3], [9], [13], [16], [19]. The high carrier concentration can be attributed to the presence of impurities and donor defects in the material. In addition, the use of glass as a substrate contributes to the generation of these defects, influencing the observed free carrier concentration [5], [27].
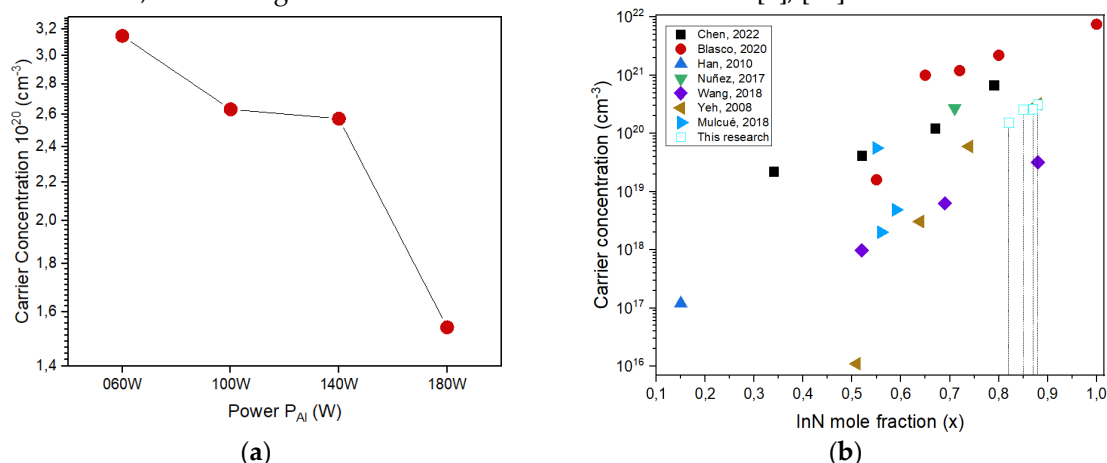

Figure 13. Variation of Free Carrier Concentration in InAlN Layers with Target Power. (a) This research; (b) Comparison with other reports.

Figure 14 illustrates how the resistivity of the InAlN layers varies as a function of the power applied to the aluminum target. An increase in resistivity is observed as power increases, reflecting a decrease in the electrical conductivity of the material. This behavior is attributed to the intrinsic properties of AlN, which is more resistive compared to InN. As a result, the electrons in the material

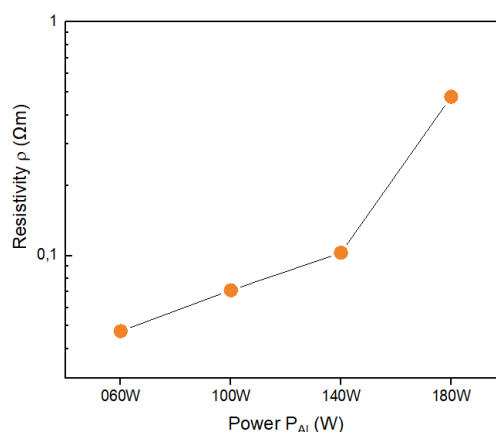are more confined, which reduces their mobility and thus the electrical conductivity of the semiconductor.

Figure 14. Increase of Resistivity in InAlN Layers with Increase of Aluminum Target Power.

Figure 15 shows how the free carrier mobility (μ) varies as a function of the power applied to the aluminum target. It is observed that μ decreases with increasing power, indicating that the electrons find it more difficult to move inside the material. The μ values obtained range from 14.01 to 0.16cm²/Vs, figures that, although low, are within the range reported in the literature for InAlN. One of the factors affecting carrier mobility is the high dispersion in peak heights on the surface, which increases roughness and reduces free movement
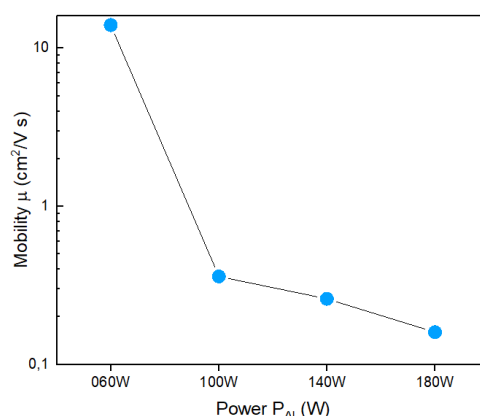

Figure 15. Decrease in InAlN Mobility with Target Power.

5. Conclusions

The research presented demonstrates significant advances in the fabrication of indium aluminum nitride (InAlN) layers by the DC co-sputtering method at room temperature. This innovative approach has overcome previous challenges associated with the synthesis of this material, particularly in terms of cost reduction and improved efficiency in the production of optoelectronic devices and solar cells.

The results obtained indicate that it is possible to tune the stoichiometry of InAlN by varying the power applied to the aluminum target, which directly influences the optical, electrical and morphological properties of the material. It has been shown that an increase in the power of the aluminum target leads to a higher incorporation of aluminum and nitrogen into the layers, favoring the formation of AlN. This is reflected in an increase in bandgap, a decrease in the concentration of free carriers and an increase in the resistivity of the material, which is consistent with the intrinsic properties of AlN.

Furthermore, morphological analysis by AFM revealed that the fabricated InAlN layers exhibit exceptionally smooth surfaces, with roughness values below 3nm, which is desirable for the fabrication of interfaces with low defect density. This aspect is crucial for improving the efficiency of devices such as solar cells, where surface uniformity and quality are determining factors.

Conflicts of Interest: "The authors declare no conflicts of interest.". "The funders had no role in the design of the study; in the collection, analyses, or interpretation of data; in the writing of the manuscript; or in the decision to publish the results".

References

1. W. Lv et al., "Mechanical properties of single-phase Al1−xInxN films across the compositional range (0 ≤ x ≤ 0.7) grown by radio-frequency magnetron sputtering," *Appl Surf Sci*, vol. 504, Feb. **2020**, doi: 10.1016/j.apsusc.2019.144335.
2. H. He *et al.*, "Band gap energy and bowing parameter of In-rich InAlN films grown by magnetron sputtering," *Appl Surf Sci*, vol. 256, no. 6, pp. 1812–1816, Jan. **2010**, doi: 10.1016/j.apsusc.2009.10.012.
3. R. Blasco, S. Valdueza-Felip, D. Montero, M. Sun, J. Olea, and F. B. Naranjo, "Low-to-Mid Al Content (x = 0–0.56) AlxIn1−xN Layers Deposited on Si(100) by Radio-Frequency Sputtering," *Phys Status Solidi B Basic Res*, vol. 257, no. 4, **2020**, doi: 10.1002/pssb.201900575.
4. M. D. Smith *et al.*, "A comparison of the 60 Co gamma radiation hardness , breakdown characteristics and the effect of SiN x capping on InAlN and AlGaN HEMTs for space applications," *Semicond Sci Technol*, vol. 31, no. 2, p. 25008, doi: 10.1088/0268-1242/31/2/025008.
5. L. F. Mulcué-Nieto, W. Saldarriaga, W. de la Cruz, E. Restrepo, M. S. Ospina, and D. Escobar, "Study of InAlN thin films deposited on silicon, ITO/PET, and ITO/GLASS substrates at room temperature for its possible use in solar cells," *Journal of Materials Science: Materials in Electronics*, vol. 33, no. 3, pp. 1162–1172, Jan. **2022**, doi: 10.1007/s10854-021-07398-w.
6. A. Núñez-Cascajero *et al.*, "In-rich AlxIn1-xN grown by RF-sputtering on sapphire: From closely-packed columnar to high-surface quality compact layers," *J Phys D Appl Phys*, vol. 50, no. 6, Jan. **2017**, doi: 10.1088/1361-6463/aa53d5.
7. T. Peng, J. Piprek, G. Qiu, J. O. Olowolafe, and K. M. Unruh, "Band gap bowing and refractive index spectra of polycrystalline AlxIn1−xN films deposited by sputtering.," *Appl Phys Lett*, vol. 2439, **1997**, doi: 10.1063/1.120112.
8. C. J. Dong *et al.*, "Growth of well-oriented AlxIn1−x N films by sputtering at low temperature," *Journal of Alloys and Compounds journal*, vol. 479, pp. 812–815, **2009**, doi: 10.1016/j.jallcom.2009.01.075.
9. M. Sun *et al.*, "Comparison of the Material Quality of AlxIn1−xN (x—0–0.50) Films Deposited on Si(100) and Si(111) at Low Temperature by Reactive RF Sputtering," *Materials*, vol. 15, no. 20, Oct. **2022**, doi: 10.3390/ma15207373.
10. H. F. Liu, C. C. Tan, G. K. Dalapati, and D. Z. Chi, "Magnetron-sputter deposition of high-indium-content n-AlInN thin film on p-Si(001) substrate for photovoltaic applications," *J Appl Phys*, vol. 112, no. 6, **2012**, doi: 10.1063/1.4754319.
11. Garzon-Fontecha Angelica; Castillo Harvi; Curiel Mario; Montaño-Figueroa Ana; Quevedo-Lopez Manuel; De La Cruz Wencel, "SnOx thin films tunable conductivity for fabrication of p-n homo-junction," *Surface and interface Analysis*, **2020**, doi: 10.1002/sia.6873.
12. Q. Guo, T. Tanaka, M. Nishio, and H. Ogawa, "Optical bandgap energy of wurtzite in-rich AlInN alloys," *Japanese Journal of Applied Physics, Part 2: Letters*, vol. 42, no. 2 B, **2003**, doi: 10.1143/JJAP.42.L141.
13. W. Song, T. Li, L. Zhang, W. Zhu, and L. Wang, "Influence of growth parameters on microstructures and electrical properties of InxAl1−xN thin films using sputtering," *J Alloys Compd*, vol. 885, Dec. **2021**, doi: 10.1016/j.jallcom.2021.160977.
14. M. Miyoshi, Y. Kuraoka, M. Tanaka, and T. Egawa, "Metalorganic chemical vapor deposition and material characterization of lattice-matched InAlN/GaN two-dimensional electron gas heterostructures," *Applied Physics Express*, vol. 1, no. 8, pp. 0811021–0811023, Aug. **2008**, doi: 10.1143/APEX.1.081102.

15. M. Alizadeh *et al.*, "Photoelectrochemical behavior of AlxIn1-xN thin films grown by plasma-assisted dual source reactive evaporation," *J Alloys Compd*, vol. 670, pp. 229–238, Jun. **2016**, doi: 10.1016/j.jallcom.2016.02.056.

16. L. F. Mulcué-Nieto, C. D. Acosta-Medina, W. Saldarriaga, and S. Mendoza, "Structural, morphological , electrical and optical properties of amorphous InxAl1-xN thin films for photovoltaic applications," *J Non Cryst Solids*, vol. 499, no. January **2019**, pp. 328–336, **2018**, doi: 10.1016/j.jnoncrysol.2018.07.047.

17. J. A. Pérez Taborda, J. C. Caicedo, M. Grisales, W. Saldarriaga, and H. Riascos, "Deposition pressure effect on chemical, morphological and optical properties of binary Al-nitrides," *Opt Laser Technol*, vol. 69, pp. 92–103, **2015**, doi: 10.1016/j.optlastec.2014.12.009.

18. S. Valdueza-Felip, R. Blasco, J. Olea, A. Díaz-Lobo, A. F. Braña, and F. B. Naranjo, "AlxIn1-xN on Si (100) Solar Cells (x = 0-0.56) deposited by RF sputtering," *Materials*, vol. 13, no. 10, May 2020, doi: 10.3390/ma13102336.

19. A. Núñez-Cascajero *et al.*, "Study of high In-content AlInN deposition on p-Si(111) by RF-sputtering," *Jpn J Appl Phys*, vol. 55, no. 5, **2017**, doi: 10.7567/JJAP.55.05FB07.

20. G. Perillat-merceroz, G. Cosendey, J. Carlin, R. Butté, and N. Grandjean, "Intrinsic degradation mechanism of nearly lattice-matched InAlN layers grown on GaN substrates Intrinsic degradation mechanism of nearly lattice-matched InAlN layers grown on GaN substrates," vol. 063506, **2013**, doi: 10.1063/1.4790424.

21. PVEducation.org, "Absorption Coefficient," https://www.pveducation.org/pvcdrom/pn-junctions/absorption-coefficient. Accessed: Apr. 28, **2024**. [Online]. Available: https://www.pveducation.org/pvcdrom/pn-junctions/absorption-coefficient

22. T. Aschenbrenner *et al.*, "Optical and structural characterization of AlInN layers for optoelectronic applications," *J Appl Phys*, vol. 108, no. 6, Sep. **2010**, doi: 10.1063/1.3467964.

23. J. J. Chen, D. L. Qi, X. F. Li, J. Y. Song, and L. H. Shen, "Optical and electrical properties of Al1-xInxN films with a wide middle-composition range by RF sputtering," *Appl Phys A Mater Sci Process*, vol. 128, no. 2, Feb. **2022**, doi: 10.1007/s00339-022-05289-3.

24. G. Fonthal, L. Tirado-Mejía, J. I. Marín-Hurtado, H. Ariza-Calderón, and J. G. Mendoza-Alvarez, "Temperature dependence of the band gap energy of crystalline CdTe."**2024** [Online]. Available: www.elsevier.nl/locate/jpcs

25. A. Oliva, O. Solís-Canto, R. Castro-Rodrıguez, P. Quintana, and M. Mexicó, "Formation of the band gap energy on CdS thin films growth by two different techniques.," **2001**.

26. K. Nakamura, A. Kobayashi, K. Ueno, J. Ohta, and H. Fujioka, "AlN/InAlN thin-film transistors fabricated on glass substrates at room temperature," *Sci Rep*, vol. 9, no. 1, Dec. **2019**, doi: 10.1038/s41598-019-42822-6.

27. N. Afzal, M. Devarajan, and K. Ibrahim, "A comparative study on the growth of InAlN films on different substrates," *Mater Sci Semicond Process*, vol. 51, pp. 8–14, **2016**, doi: 10.1016/j.mssp.2016.04.004.